Metabolic changes in agrobacterium tumefaciens-infected Brassica rapa

Simoh, S.; Quintana, N.; Kim, H.K.; Choi, Y.H.; Verpoorte, R.

Journal of Plant Physiology **166** (2009) 1005—1014

Available online at www.sciencedirect.com

ScienceDirect

JOURNAL OF PLANT PHYSIOLOGY

www.elsevier.de/jplph

Metabolic changes in *Agrobacterium tumefaciens*-infected *Brassica rapa*

Sanimah Simoh[a,b], Naira Quintana[a], Hye Kyong Kim[a], Young Hae Choi[a,*], Robert Verpoorte[a]

[a]*Division of Pharmacognosy, Section Metabolomics, Institute of Biology, Leiden University, Einsteinweg 55, P.O. Box 9502, 2333 CC Leiden, The Netherlands*
[b]*Biotechnology Research Centre, Malaysian Agricultural Research and Development Institute, Kuala Lumpur, Malaysia*

Received 30 October 2008; accepted 26 November 2008

KEYWORDS
Agrobacterium tumefaciens;
Brassica rapa;
NMR spectroscopy;
Nopaline;
Octopine

Summary

Agrobacterium has the ability to transfer its genetic material, T-DNA, into the plant genome. The unique interaction between the bacterium and its host plant has been well studied at the transcriptome, but not at the metabolic level. For a better understanding of this interaction it is necessary to investigate the metabolic changes of the host plant upon infection with *Agrobacterium tumefaciens*. This study investigated the metabolic response of *Brassica rapa* to infection with disarmed and tumor-inducing strains of *A. tumefaciens* using ^{1}H nuclear magnetic resonance spectroscopy combined with multivariate data analysis. The partial least square-discriminant analysis (PLS-DA) of two varieties of *B. rapa* showed that there was a clear differentiation in the metabolite profiles of *B. rapa* leaves infected with the disarmed strain LBA4404 and with tumor-inducing octopine and nopaline strains, particularly in the flavonoid, phenylpropanoid, sugar and free amino/organic acid contents. However, individual PLS-DA of each type of infection suggests that, in general, some flavonoids and phenylpropanoids were suppressed as a consequence of these infections. The results obtained in this study indicate that the disarmed strain LBA4404 and tumor-inducing strains have different effects on the metabolite profile of *B. rapa*.

Introduction

Agrobacterium tumefaciens is a well-known plant pathogenic bacterium with the ability to deliver part of its genetic materials, the T-DNA

*Corresponding author. Tel.: +31 71 527 4471; fax: +31 71 527 4511.
E-mail address: y.choi@chem.leidenuniv.nl (Y.H. Choi).

0176-1617/$ - see front matter © 2009 Elsevier GmbH. All rights reserved.
doi:10.1016/j.jplph.2008.11.015

from its tumor-inducing (Ti) plasmid, into the genome of the host plants, which are generally dicotyledons. *Agrobacterium* possessing T-DNA incites the formation of crown gall tumors in infected plant tissue, and tumor-specific compounds, known as opines, are synthesized as a result of the expression of the T-DNA gene in the tumor cell. Opines, which are reductive conjugates of amino acids and organic acids, e.g. pyruvate and α-ketoglutarate, or glucose (Chilton et al., 2001), constitute a major carbon/nitrogen source for *Agrobacterium* (Bevan and Chilton, 1982; Nester et al., 1984). The type of opine produced is determined by the bacterial strains that incite the tumor, and octopine-, nopaline-, succinamopine- or leucinopine-specific producing strains have been reported (Hooykaas and Beijersbergen, 1994). However, the most common are octopine- (a conjugate of arginine and pyruvate) and nopaline- (a conjugate of α-ketoglutarate and arginine) producing strains.

The unique capacity of *Agrobacterium* to transfer the T-DNA into a host plant is driven by virulence genes located outside the T-DNA region. The infection is regulated by a two-component signal transduction system consisting of virulence proteins encoded by *virA* and *virG* genes. These proteins sense the chemical signal (monosaccharide and phenolic compounds such as acetosyringone) released by the wounded plant cell, leading to the activation of other virulence genes. The expression of all these genes initiates the T-DNA transfer from the *Agrobacterium* to the host genome. Another component, a set of virulence (*chv*) genes located in the bacterial chromosome, is involved in bacterial chemotaxis and attachment to the wounded plant host. Plant host proteins also play a key role in this infection process (Gelvin, 2000). Upon integration of the T-DNA into the plant nuclear genome, the enzymes for the biosynthesis of auxins, cytokinins and opines are induced. The understanding of the *Agrobacterium*/plant cell interaction has had a great impact in the field of biotechnology, particularly in the plant transformation technology. For example, it can be used to insert any DNA of interest into the T-DNA, which is then transferred and integrated into the plant cell genome and subsequently expressed in the target plant. Thus far, a broad range of dicotyledons and some monocotyledons (which were considered as recalcitrant species) can now be infected by *A. tumefaciens*. Recent discoveries have shown that *Agrobacterium* transformation can be extended to non-plant eukaryotic organisms including fungi, mushrooms and human cells (reviewed by Lacroix et al., 2006).

Brassica rapa is one of the major species of the *Brassica* (Brassicaceae) genus, which includes plants such as turnip, cauliflower, cabbage, kohlrabi and brussel sprouts, all of which are important as vegetables, forage or oilseed crops (Cardoza and Stewart, 2004). These plants contain a large number of interesting phytochemicals, including some with anticancer properties (Christey and Braun, 2004). Considerable progress has been made in recent years to produce transgenic *B. rapa* with specific desired traits introduced by *Agrobacterium*-mediated transformation. However, this effort has been hampered partly by inefficient transgenic transformation and subsequent regeneration of the targeted plant tissue. Plants infected with pathogens such as *Agrobacterium* activate defense signal transduction, which results in hypersensitive response (HR) (Kuta and Tripathi, 2005), a factor thought to contribute to the inefficiency of the *Agrobacterium*-mediated transformation system (Gustavo et al., 1998). Previous studies have also shown that plant gene expression, including that of defense-related genes, was altered in response to *A. tumefaciens* infection (Ditt et al., 2001, 2005). Though the effect at the transcriptome level has been extensively studied, there is very scarce information at the metabolome level. However, a deeper understanding of the plant/*Agrobacterium* interaction requires an investigation of the metabolome changes induced in *B. rapa* upon infection with *A. tumefaciens*. The information obtained may also shed new light not only on how interaction with *Agrobacterium* affects the metabolite pool of *B. rapa*, but also on the extent to which these changes might directly or indirectly influence the transformation efficiency.

The current trend in utilizing nuclear magnetic resonance spectroscopy (NMR) as a tool for plant metabolomics results from its potential to quantify and identify diverse groups of metabolites including amino acids, carbohydrates, lipids, phenolic and terpenoids in a reduced number of steps (Choi et al., 2006; Kim et al., 2006). In our previous work, NMR-based metabolomics, using not only one-dimensional ^{1}H NMR but also 2D-NMR such as ^{1}H–^{1}H *J*-resolved, ^{1}H–^{1}H-correlated spectroscopy (COSY), heteronuclear single quantum coherence (HSQC) and heteronuclear multiple bonds coherence (HMBC), was applied to uncover metabolic alterations induced by diverse biological factors such as the presence of metals (Jahangir et al., 2008), developmental stages (Abdel-Farid et al., 2007), herbivore attack and fungal infection. This approach has allowed the identification of a wide range of *Brassica* metabolites.

On the basis of the metabolic information obtained from the previous studies, and viewing this case as a model system of plant/bacteria interaction, the study of the metabolic changes of *B. rapa* upon infection with disarmed and tumor-inducing octopine- and nopaline-strains of *A. tumefaciens* was undertaken.

Materials and methods

Plant materials and growth of *Agrobacterium*

Four different cultivars of *Brassica rapa*; Raapstelen, Herfstraap and Witte Mei, obtained from the Plant Ecology Section, Institute of Biology, Leiden University (Leiden, The Netherlands) and ssp. *oleifera* obtained from Plant Boreal Ltd. (Jokioinen, Finland) were grown from seeds and kept in greenhouse conditions, with a 16/8 h (light/dark) photoperiod at 300–500 μmole m^{-2} s^{-1}. Disarmed *Agrobacterium* strain LBA4404 carrying *entC* gene and CaMV 35S promoter and tumor-inducing *Agrobacterium* strain LBA4001 (octopine) and LBA4902 (nopaline) were used. The bacteria were inoculated in liquid LB medium (1% Bacto tryptone, 0.5% Bacto yeast extract, 0.5% NaCl) containing antibiotic rifampicin and kanamycin (50 μg/mL) and incubated overnight at 28 °C in a rotary shaker at 200 rpm in the dark before inoculation.

Inoculation of *B. rapa* with disarmed strain LBA4404

Inoculation of *B. rapa* with disarmed *Agrobacterium* LBA4404 was carried out on 6-week-old greenhouse-grown plants. Four varieties, Raapstelen, Witte Mei, Herfstraap and ssp. *oleifera* were used in this experiment. The surfaces of the first three lower leaves were first wounded with scalpel blades. Depending on the size of the leaves, 1–2 mL of bacterial cultures ($OD_{600} = 1.0$–1.5, diluted with distilled water) were sprayed uniformly on both the upper and lower sides of leaves. To evaluate the systemic effects of infection, the first two upper leaves were analyzed. The control experiments were carried out in the same way, but plants were sprayed with distilled water instead of bacterial cultures. Healthy, unwounded plants were used as a blank control. The leaves were harvested 7 days after inoculation.

Inoculation of *B. rapa* with tumor-inducing nopaline (LBA4902) and octopine (LBA4001) strains

To induce tumor growth, the stems of 3-week-old *B. rapa* plants were injected with 1 mL of bacterial cultures ($OD_{600} = 1.0$–1.5, diluted with distilled water) from tumor-inducing octopine and nopaline strains. Because of the difficulty in inducing tumor growth in cv. Hersfstraap and Witte Mei, only two varieties, i.e., cv. Raapstelen and ssp. *oleifera*, were used for this experiment. The stem below the tumors, the first two upper leaves from tumor-bearing plants, and the tumors themselves were harvested when the plants were 8 weeks old. Three individual plants were used as replicates for each experiment. The control experiments were carried out in the same way, but plants were injected with distilled water instead of bacterial cultures. Healthy, unwounded plants were used as blank controls.

Extraction of tumor and plant materials

The tumors and plant material were ground with liquid nitrogen and freeze-dried prior to extraction. Fifty milligrams of freeze-dried material were transferred to a 2-mL microtube and 750 μL of methanol-d_4 and 750 μL of KH_2PO_4 buffer in D_2O (pH 6.0 containing 0.05% of trimethyl silyl propionic acid sodium salt (TMSP, w/v) were added. The mixture was vortexed for 2 min, then sonicated for 15 min and finally centrifuged at 13,000 rpm for 20 min at room temperature. An aliquot of 800 μL of the supernatant were transferred into a 5-mm NMR tube for metabolic analysis.

NMR spectra measurement

^{1}H NMR, two-dimensional *J*-resolved spectra were recorded at 25 °C on a 500 MHz Bruker DMX-500 spectrometer (Bruker, Karlsruhe, Germany). ^{1}H–^{1}H-correlated spectroscopy (COSY), heteronuclear single quantum coherence (HSQC), and heteronuclear multiple bonds coherence (HMBC) spectra were recorded on a 600 MHz Bruker DMX-600 spectrometer (Bruker). All the NMR parameters were the same to those of our previous reports (Abdel-Farid et al., 2007; Jahangir et al., 2008).

Data analysis

Spectral intensities of ^{1}H NMR spectra were scaled to total intensity and reduced to integrated regions of equal width (0.04 ppm) corresponding to

the region of δ0.4–δ10.0. The regions of δ4.8–δ4.9 and δ3.28–δ3.40 were excluded from the analysis because of the residual signal of water and MeOH. Principal component analysis (PCA) and partial least square regression-discriminant analysis (PLS-DA) were performed with the SIMCA-P software (v. 12.0, Umetrics, Umeå, Sweden).

Results

A. tumefaciens infection

The leaves of all varieties of 6-week-old *B. rapa* plants that had been sprayed with the disarmed *Agrobacterium* strain LBA4404 did not exhibit any obvious visible effect. A few leaves produced a slight yellowish color 7 days after treatment. In the case of infection with tumor-inducing nopaline- or octopine-strains, only two of the *B. rapa* plants evaluated in this study, var. Raapstelen and ssp. *oleifera*, started to form tumors 1 week after infection. However, the tumor formation was observed only in 3-week-old infected plants, while no tumors were induced when 6-week-old plants were infected. Consequently, in the case of tumor-inducing strains, we infected only the 3-week-old plants. Tumors induced by the nopaline strain have a smooth morphology, whereas tumors induced by the octopine strain have a rough morphology (Hooykaas et al., 1980) as shown in Supplementary Figure 1.

^{1}H NMR metabolic analysis of *B. rapa* infected with disarmed and tumor-inducing strain of *A. tumefaciens*

For the identification of *B. rapa* metabolites, ^{1}H NMR and diverse two-dimensional spectra (*J*-resolved, ^{1}H–^{1}H-COSY, HSQC and HMBC), were used, as was our in-house database of reference compounds and results of previous studies (Abdel-Farid et al., 2007; Jahangir et al., 2008). The compounds detected in this study were free amino- and organic acids such as alanine, valine, threonine, arginine, leucine, isoleucine, succinic acid, fumaric acid, formic acid, glutamic acid and malic acid. Glucose and sucrose were the carbohydrates detected. As for secondary metabolites, the signals of the aliphatic glucosinolate (progoitrin), the flavonoids (quercetin and kaempferol), and the phenylpropanoids (sinapoyl- and coumaroyl malate) were also detected. Other compounds identified were adenine and choline.

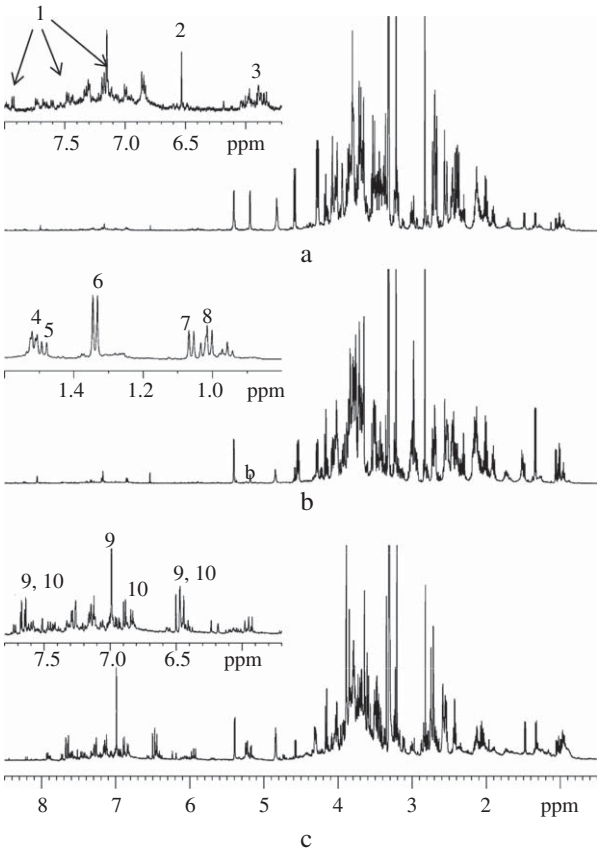

Figure 1. Typical ^{1}H NMR spectra of (a) nopaline tumor (b) octopine tumor (c) disarmed *Agrobacterium* (LBA4404) infected *Brassica rapa* Raapstelen leaf: 1 – indole-3-acetic acid, 2 – fumaric acid, 3 – progoitrin, 4 – octopine, 5 – alanine, 6 – threonine, 7 – valine, 8 – leucine/isoleucine, 9 – sinapoyl malate, 10 – coumaroyl malate.

Visual inspection of the ^{1}H NMR spectra allowed the identification of some of the metabolites specifically induced by disarmed or tumor-inducing strains of *Agrobacterium*. With the aid of *J*-resolved and ^{1}H–^{1}H-COSY spectra as well as comparison with the spectra of octopine reference compound, the signals at δ1.51 (d, $J = 8.0$, H-3′), δ3.68 (m, H-2, H-2′), δ1.90 (m, H-3), δ1.70 (m, H-4), and δ3.24 (t, $J = 8.0$, H-5) in octopine-induced tumors were attributed to the presence of octopine. However, the signal of nopaline could not be detected in the samples of tumors induced by the nopaline strain. The signals of sinapoyl malate at δ6.48 (dd, $J = 16.0$ Hz) and δ6.99 (s), and quercetin were present in both the nopaline and octopine tumors, while arginine, indole acetic acid (IAA) and progoitrin were detected exclusively in nopaline tumors. Flavonoids (kaempferol and quercetin) and phenylpropanoids (sinapoyl malate and coumaroyl malate) were identified in disarmed strain LBA4404-infected leaves and in the leaves and

stems of the tumor-bearing plants. The typical ^{1}H NMR spectra of nopaline and octopine tumors and of disarmed LBA4404-infected leaves are shown in Figure 1.

Multivariate data analysis of the ^{1}H NMR spectra from both disarmed strain LBA4404-infected leaves and leaves removed from tumor-bearing plants

In order to obtain a detailed metabolic differentiation of the two types of *A. tumefaciens* infection, principal component analysis (PCA) was initially performed for ^{1}H NMR data of the plants infected with disarmed and tumor-inducing strains of *A. tumefaciens*. For the disarmed strain LBA4404, local infected leaves were studied, whereas for tumor-inducing strains, leaves from the tumor-bearing plant were used. Unfortunately, PCA results did not show any clear separation (data not shown). Unsupervised methods such as PCA might not be optimal for pattern recognition because they separate samples based on overall variance, which means that all chemical noise or random unrelated variation of metabolites are also considered to obtain the maximum separation among all samples (Kind et al., 2007). To overcome the limitation posed by PCA, the supervised method PLS-DA was applied. For PLS-DA, the data obtained from leaf samples were divided into four classes according to the infecting microbe: (1) tumor-inducing octopine strain infected plants, (2) tumor-inducing nopaline strain infected plants, (3) disarmed strain LBA4404 infected plants, and (4) leaves from control plants for comparison with both tumor-inducing octopine/nopaline strains and disarmed strain LBA4404 (blank controls and plants injected with distilled water only). The score plot (Figure 2a) of PLS-DA shows a distinct separation between the leaves infected with disarmed strain LBA4404 (group 3) and those from tumor-bearing plants (groups 1 and 2), and the control samples (group 4) clustered together. Investigation of the loading plot (Figure 2b) indicated that leaves infected with disarmed strain LBA4404 had a higher concentration of phenylpropanoids, including sinapoyl- and coumaroyl malate, and of glucose and sucrose, alanine, and isoleucine/leucine. In contrast, the leaves taken from tumor-bearing plants after infection with octopine- and nopaline-strains (located in the positive side of PC3) accumulated higher levels of the flavonoids quercetin and kaempferol, and some free amino- and organic acids, i.e., valine, threonine, glutamic acid, succinic acid, formic acid and malic acid. The

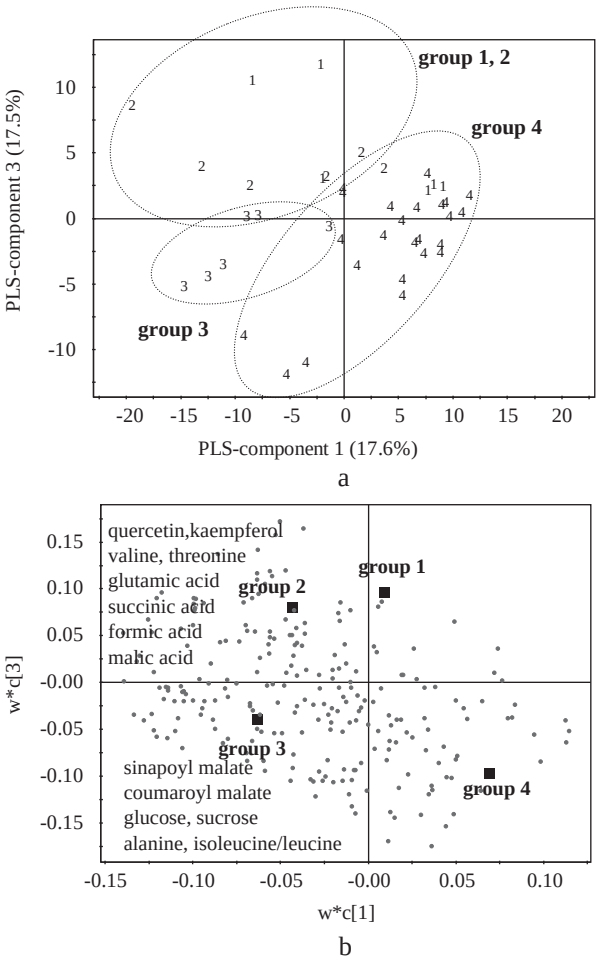

Figure 2. PLS-DA score plot (a) and loading plot (b) of two varieties of *Brassica rapa* leaves infected with disarmed strain LBA4404 and the leaves taken from tumor-bearing plants (PLS-component 1 vs. PLS-component 3): 1 – leaves from plant infected with octopine-inducing strain, 2 – leaves from plant infected with nopaline-inducing strain, 3 – leaves infected with disarmed strain LBA4404, 4 – controls (blank controls and plants injected with only distilled water).

relative ^{1}H NMR intensities of the altered metabolites is shown in Table 1. Although the plants were infected at two different ages (3 weeks old for the plants infected with tumor-inducing strains, and 6 weeks old for leaves infected with disarmed strain LBA4404), this did not appear to be the cause of the separation since all the control and blank leaf samples clustered together independent of age.

Identification of *B. rapa* metabolites affected by tumor-inducing strains of *A. tumefaciens* using multivariate data analysis

PLS-DA was then applied individually to samples from plants infected with all three strains in order

Table 1. Relative ^{1}H NMR intensities[a] of changed metabolites in the leaves of the *Brassica rapa* plant after infection with disarmed and tumor-inducing strain of *Agrobacterium tumefaciens*.

Name of metabolites	Target resonances	var. Raapstelen			ssp. *oleifera*		
		Disarmed	Tumor-inducing		Disarmed	Tumor-inducing	
			Nopaline	Octopine		Nopaline	Octopine
Alanine	δ1.48	159.26	281.70	152.78	305.63	106.41	66.74
Valine	δ1.04	185.22	215.03	154.78	189.16	115.22	106.31
Threonine	δ1.32	137.41	177.0	96.94	174.44	111.69	80.85
Isoleucine/leucine	δ0.96	251.95	194.92	122.08	465.40	112.56	95.01
Valine	δ1.05	224.51	315.28	188.85	358.19	136.74	105.43
Glutamic acid	δ2.08	134.68	392.37	243.54	226.19	196.08	111.20
Succinic acid	δ2.52	140.14	38.38	118.82	142.98	275.71	90.0
Fumaric acid	δ6.56	69.63	67.2	58.72	89.31	74.38	79.32
Malic acid	δ4.32	124.55	190.42	62.23	106.95	106.49	102.34
Indole-3-acetic acid	δ7.72	147.02	304.65	390.79	10.82	80.23	80.26
Adenine	δ8.20	82.73	140.51	118.28	136.96	83.54	89.25
Glucose	δ4.60	110.83	51.66	152.79	161.43	49.68	149.25
Sucrose	δ5.40	133.73	35.77	44.48	10.86	73.0	60.05
Kaempferol	δ7.96	110.28	121.65	84.54	90.27	136.25	97.5
Quercetin	δ6.76	75.82	154.88	108.27	137.96	102.55	87.23
Sinapoyl malate	δ6.96	62.96	123.74	77.26	144.44	67.95	73.59
Coumaroyl malate	δ6.84	73.75	116.52	91.93	147.27	88.93	81.49

[a]All intensities were normalized 100% of control plants.

to clearly identify the metabolites affected by each infection. First, in order to find metabolites induced by tumor-inducing *A. tumefaciens*, PLS-DA for the plant infected with tumor-inducing strains was divided into three classes: (1) tumors induced by octopine and nopaline strains, (2) leaves and stems from the plant infected with octopine and nopaline strains, (3) leaves and stems from healthy plants including the plants injected with distilled water and those without any treatment. The score plot (PLS-component 2 vs. PLS-component (4) of PLS-DA, shown in Figure 3a, illustrates clear discrimination among the three different groups. The corresponding signals in the loading plot (Figure 3b) suggest that the tumors induced by the nopaline- and octopine-strain had higher concentrations of succinic acid and glutamic acid. The leaves/stems of tumor-bearing plants showed higher accumulations of alanine, threonine, leucine/isoleucine, formic acid and adenine. Conversely, the leaves/stems from control plants (without any treatment and injected with only distilled water) were found to have higher concentrations of fumaric and malic acid, kaempferol, and quercetin analogues, sinapoyl- and coumaryl malate, as well as glucose and sucrose.

Identification of *B. rapa* metabolites affected by the disarmed strain LBA4404 of *A. tumefaciens*, using multivariate data analysis

The PLS-DA score and loading plots of *B. rapa* leaves infected with the disarmed strain LBA4404 of *A. tumefaciens* can be seen in Figure 4. In the score plot (PLS-component 1 vs. PLS-component 2) (Figure 4a), a distinct separation was found between the local infected leaves and their controls, while no separation between the systemic leaves and their controls was observed. Investigation of the corresponding loading plot (Figure 4b) revealed that the signals with the highest impact in local infected leaves were all amino acids (alanine, threonine, valine and glutamic acid), whereas the signals responsible for control plants were flavonoids (quercetin and kaempferol analogues), phenylpropanoids (sinapoyl malate and coumaroyl malate) and formic acid. Also, the loading plot clearly shows that the negative side of PLS component 2, corresponding to local infected leaves, is dominated by the signals of compounds in the aliphatic region, including amino and organic acids. The positive side of PLS component 2, which

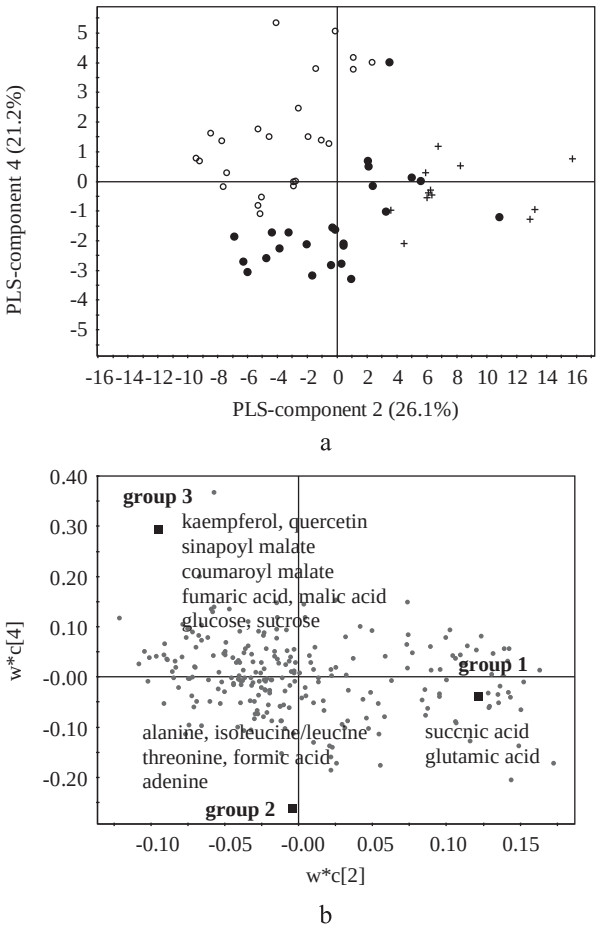

Figure 3. PLS-DA score plot (a) and loading plot (b) of *Brassica rapa* infected with tumor-inducing octopine- and nopaline-strains of *Agrobacterium tumefaciens* (PLS-component 2 vs. PLS-component 4). +; Tumors induced by octopine and nopaline strain (group 1) ●; Leaves and stems from tumor-bearing plants (group 2), ○; Leaves and stems without any treatment and leaves and stems from control plants (injected with distilled water) (group 3).

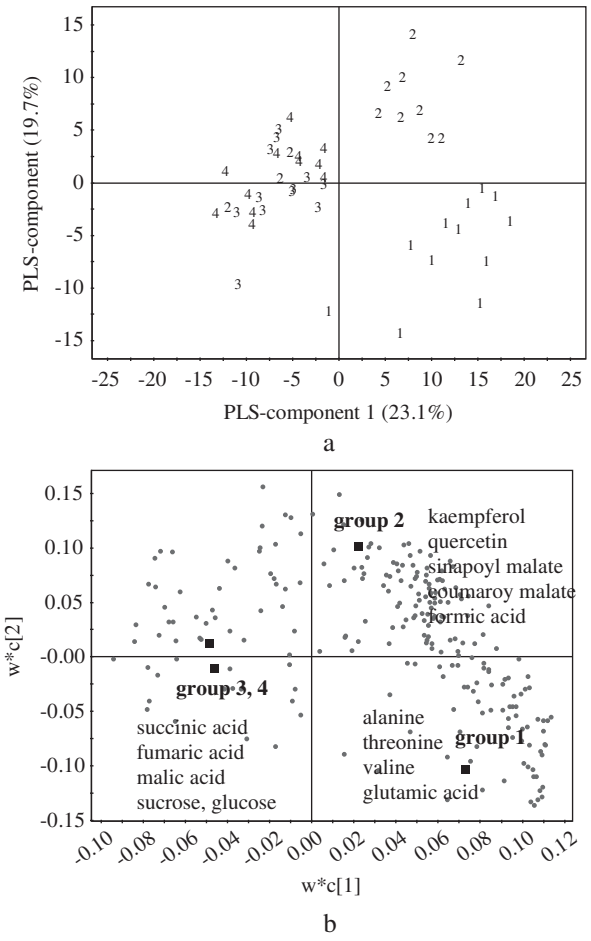

Figure 4. PLS-DA score plot (a) and loading scatter plot (b) of *Brassica* leaves infected with disarmed strain (LBA4404) of *Agrobacterium tumefaciens*: 1 – local infected leaves, 2 – control for local infected leaves, 3 – systemic leaves, 4 – control for systemic leaves.

corresponds to the control leaves, is dominated by the signals of the compounds in the aromatic region, including secondary metabolites, flavonoids and phenylpropanoids. The metabolites identified in systemic leaves and their controls are organic acids i.e. succinic acid, fumaric acid, malic acid as well as sucrose and glucose.

Metabolite differentiation between octopine and nopaline tumors

Principal component analysis (PCA) alone was sufficient to identify the distinctive metabolites present in nopaline and octopine tumors. The PCA score plot (PC2 vs. PC3) (Figure 5) clearly shows the separation between these two tumors. The corresponding signals in the loading column plot suggest

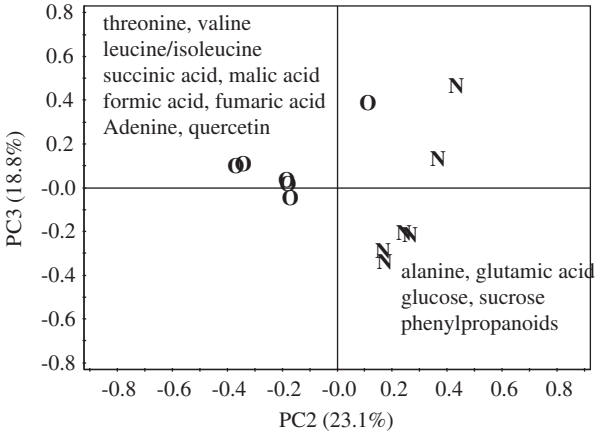

Figure 5. PCA score plot of nopaline and octopine tumors induced in *Brassica rapa* after infection with tumor-inducing nopaline and octopine strains of *Agrobacterium tumefaciens*.

that the tumors induced by the octopine-strain had higher concentrations of amino acids (threonine, valine, leucine/isoleucine), organic acids (succinic acid, malic acid, formic acid, fumaric acid), adenine and the flavonoid quercetin, whereas the tumors induced by the nopaline-strain had higher concentrations of alanine, glutamic acid, glucose, sucrose and phenylpropanoid derivatives.

Discussion

The two-dimensional spectroscopy-aided analysis of the ^{1}H NMR spectra showed that IAA, arginine and progoitrin were present exclusively in the tumors induced by the nopaline strains. Crown gall tumors have been reported to contain high levels of auxins, such as IAA and cytokinins, synthesized by the enzymes encoded by the T-DNA that is integrated into the genome of the host plant (Weiler and Kurt, 1981). Moreover, tumor growth is thought to depend on the overproduction of auxins (Schwalm et al., 2003). These compounds, together with cytokinins, ethylene and abscisic acid, are involved in the proliferation and vascularization of tumor tissue (Veselov et al., 2003) needed to efficiently provide a supply of the necessary nutrients and water. Liu and Nester (2006) suggested that IAA not only acts as an inhibitor of *vir* gene expression when it is no longer needed, but might also function as a metabolite that can serve as a chemical agent in plant defense against a wide variety of plant-associated bacteria in the rhizosphere. As the nopaline tumor is formed by the direct condensation of arginine and α-ketoglutaric acid and the octopine tumor results from condensation between arginine and pyruvic acid (Christou et al., 1986), arginine is expected to be present in crown gall tumors. However, in our case, arginine was found only in nopaline tumors, while α-ketoglutaric acid and pyruvic acid were not detected in the respective tumors.

In order to evaluate the metabolite differentiation resulting from the infection by the disarmed and tumor-inducing strains, a PLS-DA was performed (Figure 2). Only two varieties – cv. Raapstelen and ssp. *oleifera* – were chosen for this analysis. The results showed that the leaves infected with disarmed strain LBA4404 had higher concentrations of phenylpropanoids (*cis*- and *trans*-sinapoyl malate and coumaroyl malate), sugars, and some amino and organic acids than leaves obtained from tumor-bearing plants, which had higher concentrations of mostly amino and organic acids. This suggests that disarmed strain LBA4404 and tumor-inducing strains exert different influences on the metabolite profiles of *B. rapa*. Moreover, plants that have been attacked by the pathogens also activate self-defense mechanisms, for example, by producing defense compounds such as flavonoids, phenylpropanoids and glucosinolates, which protect them from a subsequent attack. This might also explain the presence of the glucosinolate, progoitrin in the nopaline tumor and flavonoid (quercetin) and phenylpropanoid derivatives in both octopine and nopaline tumors. In previous work on *Agrobacterium*-transformation of white clover (*Trifolium repens* (L)) with β-glucuronidase (*GUS*)-fused auxin-responsive promoter (GH3), Schwalm et al. (2003) showed that the plant tumors induced by *A. tumefaciens* accumulated considerable amounts of auxins, kaempferol and other flavonoid aglycones, namely, 7,4′-dihydroflavone (DHF), formononetin and medicarpin. However, none of these flavonoids were detected in our study.

PLS-DA was then applied individually to results of the leaves infected with disarmed strain LBA4404 and the plants infected with tumor-inducing octopine and nopaline strains. In the first case, 4 *B. rapa* varieties were used (cv. Raapstelen, Witte Mei, Herfstraap and ssp. *oleifera*) and their leaves were infected with disarmed strain LBA4404 when plants were 6 weeks old. Because it was difficult to incite tumor formation in cv. Herfstraap and Witte Mei, only 3-week-old cv. Raapstelen and ssp. *oleifera* plants were used for the study of the infection with tumor-inducing strains. Results of our PLS-DA showed that the infection of *B. rapa* leaves with the disarmed strain of *A. tumefaciens* suppressed the accumulation of flavonoids and phenylpropanoids. This indicates that, although the infection by disarmed strain LBA4404 was considered mild and did not have any severe effect on the infected leaves, it still caused a disruption in some metabolite levels, including certain phenylpropanoids and flavonoids. Conversely, the systemic infection of the leaves did not cause any alteration in flavonoids and phenylpropanoids when compared to the controls. The mildness of the infection might also explain why no induction of any phenylpropanoids or flavonoids was detected in the systemic leaves. The results also demonstrated that there was suppression of flavonoids and phenylpropanoids compared to the control plants (injected with only distilled water) in the leaves and stem removed from tumor-bearing plants. This indicates that *A. tumefaciens* might be able to suppress the accumulation of certain flavonoids and phenylpropanoids, compounds that are usually induced in the plants in response to biotic and a biotic stress. Finally, PCA was also used to investigate any

potential differences between the control plants (injected with only distilled water) and healthy leaves (blank control). The analysis showed that there was greater induction of flavonoids, phenylpropanoids, and amino and organic acids in control plants compared to the healthy leaves (blank controls) (data not shown).

Plants exposed to stress such as pathogen infection or mechanical wounding showed many distinct biochemical changes including the metabolites originated from phenylpropanoid pathways (Dixon and Paiva, 1995; Richard et al., 2000). These compounds are produced either at the site of infection or systemically in unwounded tissue (Ryan, 1990; Richard et al., 2000). The carbon flow is diverted from primary metabolism towards phenylpropanoid metabolism which leads, among other things, to the biosynthesis of phenylpropanoid-derived compounds (Ellard-Ivey and Doughlas, 1996). The presence of certain flavonoids and phenylpropanoid and the fluctuation of levels of primary metabolites (sugars and amino/organic acids) in the plants caused by mechanical wounding and in nopaline and octopine tumors are in line with this hypothesis. In the past years, many studies have demonstrated the role of hydroxycinnamic acid derivatives in plant defense response to biotic or abiotic stress (Daayf et al., 2000; Janas et al., 2000). Housti et al. (2002) reported the accumulation of caffeoyl malate, feruloyl malate and *p*-coumaroyl malate in the leaves of *Thunbergia alata* when these plants were treated with salicylic acid and upon local or systemic wounding. In contrast, our results from the leaves infected with disarmed strain of *A. tumefacines* suggest the suppression of flavonoids and phenylpropanoids. The leaves and stem taken from tumor-bearing plants infected with octopine- and nopaline-strains also showed a similar pattern compared to the leaves infected with disarmed strain LBA4404, even when the plants were infected at different ages. Similar results were reported by Hagemeier et al. (2001), who observed the absence of phenylpropanoid compounds when *Arabidopsis thaliana* was infected with *Pseudomonas syringae*. Furthermore, Tan et al. (2001), observed a decrease of prominent phenylpropanoid metabolites by using the same species of *Arabidopsis* and pathogen, but several cell wall-bound phenylpropanoids increased at the same time.

Acknowledgement

The authors thank Prof. P.J.J. Hooykaas for providing the different strains of *Agrobacterium*.

Appendix A. Supplementary materials

The online version of this article contains additional supplementary data. Please visit doi:10.1016/j.jplph.2008.11.015.

References

Abdel-Farid IB, Kim HK, Choi YH, Verpoorte R. Metabolic characterization of *Brassica rapa* leaves by NMR spectroscopy. J Agric Food Chem 2007;55:7936–43.

Bevan MW, Chilton MD. T-DNA of the *Agrobacterium* Ti and Ri plasmid. Annu Rev Genet 1982;16:357–84.

Cardoza V, Stewart NJR. *Brassica* biotechnology: progress in cellular and Molecular Biology. In Vitro Cell Dev Biol Plant 2004;40:542–51.

Chilton WS, Petit A, Chilton MD, Dessaux Y. Structure and characterization of the crown gall opines heliopine, vitopine and rideopine. Phytochemistry 2001;58:137–42.

Choi YH, Kim HK, Linthorst HJM, Hollander JC, Kefeber AWM, Erkenlens C, et al. NMR metabolomics to revisit the tobacco mosaic virus infection in *Nicotiana tabacum* leaves. J Nat Prod 2006;69:742–8.

Christey MC, Braun R. Production of transgenic vegetable *Brassica*. In: Nagata T, Widholm JM, Lörz H, editors. Biotechnology in agriculture and forestry. Heidelberg: Springer; 2004. p. 169–90.

Christou P, Platt SG, Ackerman MC. Opine synthesis in wild-type plant tissue. Plant Physiol 1986;82:218–21.

Daayf F, Ongena M, Boulanger R, El Hadrami I, Bélanger RR. Induction of phenolic compounds in two cultivars of cucumber by treatment of healthy and powdery mildew-infected plants with extracts of *Reynoutria sachalinensis*. J Chem Ecol 2000;26:1579–93.

Ditt RF, Nester EW, Comai L. Plant gene expression response to *Agrobacterium tumefaciens*. Proc Natl Acad Sci USA 2001;98:10954–9.

Ditt RF, Nester E, Comai L. The plant cell defense and *Agrobacterium tumefaciens*. FEMS Microb Lett 2005;247:207–13.

Dixon RA, Paiva NL. Stress-induced phenylpropanoid metabolism. Plant Cell 1995;7:1085–97.

Ellard-Ivey M, Doughlas CJ. Role of jasmonates in elicitor- and wound-inducible expression of defense genes in parsley and transgenic tobacco. Plant Physiol 1996;112:183–92.

Gelvin SB. *Agrobacterium* and plant genes involved in T-DNA transfer and integration. Annu Rev Plant Physiol Plant Mol Biol 2000;51:223–56.

Gustavo AR, Gonzalez-Cabrera J, Vazquez-Padron R, Ayra-Pardo C. *Agrobacterium tumefaciens*: a natural tool for plant transformation. Plant Biotechnol 1998;1:118–33.

Hagemeier J, Scheider B, Oldham NJ, Hahlbrock K. Accumulation of soluble and wall-bound indolic metabolites in *Arabidopsis thaliana* leaves infected

with virulent or avirulent *Pseudomonas syringae* pathovar tomato strains. Proc Natl Acad Sci USA 2001; 98:753–8.

Hooykaas PJJ, Beijersbergen AGM. The virulence system of *Agrobacterium tumefaciens*. Annu Rev Phytopathol 1994;32:157–79.

Hooykaas PJJ, Dulk-Ras HD, Oom G, Schiperoort RA. Interactions between octopine and nopaline plasmids in *Agrobacterium tumefaciens*. J Bacteriol 1980;143: 1295–306.

Housti F, Andary C, Gargadennec A, Amssa M. Effects of wounding and salicylic acid on hydroxycinnamoylmalic acid in *Thunbergia alata*. Plant Physiol Biochem 2002;40:761–9.

Jahangir M, Kim HK, Choi YH, Verpoorte R. Metabolomic response of *Brassica rapa* submitted to pre-harvest bacterial contamination. Food Chem 2008;107:362–8.

Janas KM, Cvikrová M, Palagiewicz A, Eder J. Alterations in phenylpropanoid contents in soybean roots during low temperature acclimation. Plant Physiol Biochem 2000;38:587–93.

Kim HK, Choi YH, Verpoorte R. Metabolomic anaylsis of *Catharanthus* roseus using NMR and principal component analysis. In: Saito K, Dixon RA, Willmitzer L, editors. Plant metabolomics: biotechnology in agricultural and forestry. Heidelberg: Springer; 2006. p. 261–76.

Kind T, Tolstikov V, Fiehn O, Weiss RH. A comprehensive urinary metabolomic approach for identifying kidney cancer. Anal Biochem 2007;363:185–95.

Kuta DD, Tripathi L. *Agrobacterium*-induced hypersensitive necrotic reaction in plant cells: a resistance response against *Agrobacterium*-mediated DNA transfer. African J Biotechnol 2005;4:752–7.

Lacroix B, Tzfira T, Vainstein A, Citovsky V. A case of promiscuity: *Agrobacterium*'s endless hunt for new partners. Trends Gen 2006;22:29–37.

Liu P, Nester EW. Indoleacetic acid, a product of transferred DNA, inhibits vir gene expression and growth of *Agrobacterium tumefaciens* C58. Proc Natl Acad Sci USA 2006;103:4658–62.

Nester EW, Gordon MP, Amasino RM, Yanofsky MF. Crown gall: a molecular and physiological analysis. Annu Rev Plant Physiol 1984;35:387–413.

Richard S, Lapointe G, Rutledge RG, Seguin A. Induction of chalcone synthase expression in white spruce by wounding and jasmonate. Plant Cell Physiol 2000;41: 982–7.

Ryan C. Protease inhibitors in plants: genes for improving defenses against insects and pathogens. Annu Rev Phytopathol 1990;28:425–49.

Schwalm K, Aloni R, Langhans M, Heller W, Stich S, Ullrich CL. Flavonoid-related regulation of auxin accumulation in *Agrobacterium tumefaciens*-induced plant tumors. Planta 2003;218:163–78.

Tan J, Bednarek P, Liu J, Schneider B, Svatos A, Hahlbrock K. Universally occuring phenylpropanoid and species-specific indolic metabolites in infected and uninfected *Arabidopsis thaliana* roots and leaves. Phytochemistry 2001;65:691–9.

Veselov D, Langhans M, Hartung W, Aloni R, Feussner I, Götz C, et al. Development of *Agrobacterium tumefaciens* C58-induced plant tumors and impact on host shoots are controlled by a cascade of jasmonic acid, auxin, cytokinin, ethylene and abscisic acid. Planta 2003;216:512–22.

Weiler EW, Kurt S. Phytohormones in the formation of crown gall tumors. Planta 1981;153:326–37.